RSC Advances

PAPER

View Article Online
View Journal | View Issue

Cite this: *RSC Adv.*, 2019, **9**, 18720

Nano-kaolin/Ti^{4+}/Fe_3O_4: a magnetic reusable nano-catalyst for the synthesis of pyrimido[2,1-*b*] benzothiazoles†

Bi Bi Fatemeh Mirjalili * and Roya Soltani

Received 8th March 2019
Accepted 24th May 2019

DOI: 10.1039/c9ra01767d

rsc.li/rsc-advances

Herein, nano-kaolin/Ti^{4+}/Fe_3O_4 as a new magnetic nano-catalyst was synthesized, and its structural properties were characterized using various techniques such as Fourier transform infrared (FTIR) spectroscopy, field emission scanning electron microscopy (FE-SEM), transmission electron microscopy (TEM), X-ray diffraction (XRD), a vibrating sample magnetometer (VSM), thermogravimetric analysis (TGA) and energy-dispersive X-ray spectroscopy (EDX). This catalyst was used for the synthesis of pyrimido[2,1-*b*]benzothiazoles *via* the one-pot condensation of 2-aminobenzothiazole, an aldehyde and β-keto ester under solvent-free conditions at 100 °C. This simple protocol has many advantages such as easy workup, high product yields, short reaction times and reusability of the catalyst.

Introduction

Pyrimido[2,1-*b*]benzothiazoles are an important category of fused heterocycles, with the benzothiazole ring having diverse pharmaceutical and industrial properties.[1] These compounds have shown various biological activities such as anti-bacterial,[2] anti-tumor,[3,4] anti-inflammatory,[5,6] anti-viral,[7] anticonvulsant,[8] anti-cancer[9] and antifungal activities.[10] These compounds have been synthesized *via* the condensation reaction of 2-amino benzothiazole, β-keto ester and aldehydes. Previously, various catalysts, such as thiamine hydrochloride (VB1),[11] Fe_3O_4@nano-cellulose-TiCl,[12] nano-$TiCl_2$/cellulose,[13] nanocellulose/BF_3/Fe_3O_4,[14] nano-Fe_3O_4@SiO_2–$TiCl_3$,[15] kaolin,[16] and tetrabutylammonium hydrogen sulfate (TBAHS),[17] have been applied for the preparation of these compounds. However, the drawback of these protocols is the high cost of the catalyst.

Kaolin or hydrated aluminum silicate ($Al_2O_3 \cdot 2SiO_2 \cdot 2H_2O$)[18] has been used in numerous fields such as in the medicine, paint, ceramic, rubber, paper, petroleum and glass industries.[19] Moreover, one of the most valuable application of kaolin is as promoter in chemical industry;[20] in recent years, magnetic nanoparticles (Fe_3O_4) have been used due to their advantages such as high stability, low toxicity and easy separation from reaction media.[21–23] On the other hand, single atoms,[24–27] such as transition metal atoms and their ions,[28,29] have been widely studied and used for the promotion of organic reactions. In this study, we report the synthesis and characterization of nano-kaolin/Ti^{4+}/Fe_3O_4 for the synthesis of 4*H*-pyrimido[2,1-*b*]benzothiazoles *via* the condensation reaction of ethyl acetoacetate, aromatic aldehydes, and 2-amino benzothiazole.

Results and discussion

Herein, nano-kaolin/Ti^{4+}/Fe_3O_4 was prepared as a new catalyst in two-steps. At first, $TiCl_4$ was added to the mixture of nano-kaolin and CH_2Cl_2. The resulting white powder (nano-kaolin/Ti^{4+}) was added to the suspension of nano Fe_3O_4 in CH_2Cl_2 under the ultrasonic condition for the formation of nano-kaolin/Ti^{4+}/Fe_3O_4 as a brown magnetic powder (Scheme 1). The morphology and structure of kaolin/Ti^{4+}/Fe_3O_4 were studied by various techniques such as FTIR, FE-SEM, TEM, XRD, VSM, TGA and EDX. The FTIR spectra of kaolin, Fe_3O_4, nano-kaolin/Ti^{4+} and nano-kaolin/Ti^{4+}/Fe_3O_4 are shown in Fig. 1. The absorption bands at 3342 and 3620 cm^{-1} correspond to the stretching vibrations of the O–H bond. The band at 538 cm^{-1} is attributed to Fe/O in the Fe_3O_4 nanoparticles. The Al–O and Si–O stretching vibration bands are visible at 420–550 and 1050–1100 cm^{-1}, respectively, in the FTIR spectrum of nano-kaolin/Ti^{4+}/Fe_3O_4.

The particle size of nano-kaolin/Ti^{4+}/Fe_3O_4 was studied using field emission scanning electron microscopy (FE-SEM) and transmission electron microscopy (TEM) and found to be less than 100 nm (Fig. 2).

Energy-dispersive X-ray spectroscopy (EDS) was used to determine the percentage of elements in nano-kaolin/Ti^{4+}/Fe_3O_4 (Fig. 3). The percentage of Fe, Si, Al, Ti, Cl, O and K in nano-kaolin/Ti^{4+}/Fe_3O_4 was 37.4, 25.5, 12.6, 11.0, 8.2, 4.2 and 1.2, respectively.

Department of Chemistry, College of Science, Yazd University, Yazd, P.O.Box 89195-741, Iran. E-mail: fmirjalili@yazd.ac.ir; Fax: +98 3538210644; Tel: +98 3531232672

† Electronic supplementary information (ESI) available. See DOI: 10.1039/c9ra01767d

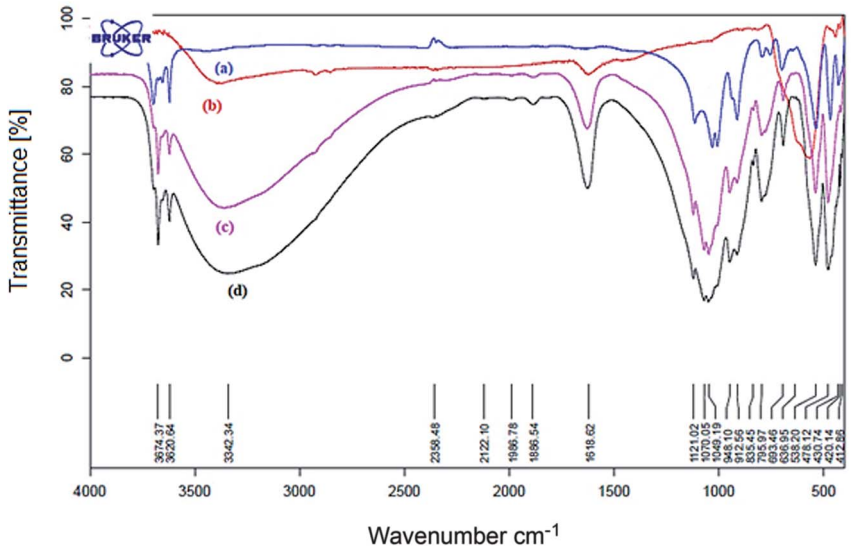

Fig. 1 FTIR spectra of (a) nano-kaolin, (b) Fe_3O_4, (c) nano-kaolin/Ti^{4+}, and (d) nano-kaolin/Ti^{4+}/Fe_3O_4.

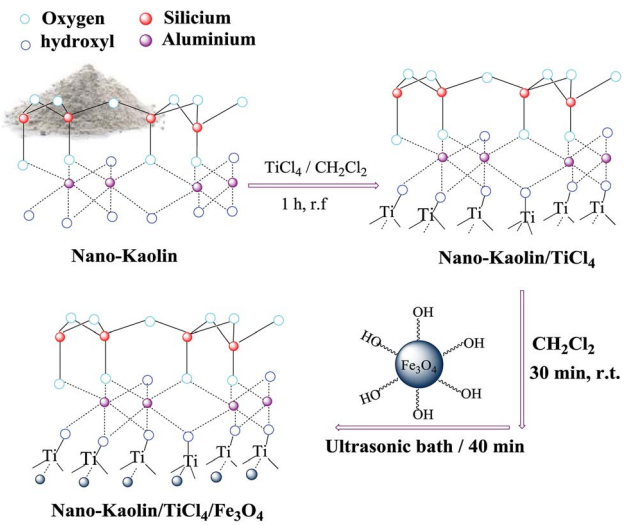

Scheme 1 Preparation of nano-kaolin/Ti^{4+}/Fe_3O_4.

The thermal stability (TG-DTA) of nano-kaolin/Ti^{4+}/Fe_3O_4 was studied by thermogravimetric analysis (TGA) in the temperature range of 50–800 °C (Fig. 4). According to Fig. 4, at 100–250 °C, the catalyst weight was reduced by 4%; this could be related to the removal of moisture and bonded water. Moreover, the catalyst lost 80% of its weight in the temperature range of 250–600 °C probably due to the collapse of the kaolin network. According to the TGA curve, this catalyst is stable up to 230 °C and suitable for reactions that are carried out at temperatures below 230 °C.

The vibrating sample magnetometer (VSM) pattern of the catalyst at room temperature shows that the coercivity value is zero, and there is no hysteresis loop and remanence; this confirms the catalytic superparamagnetic property (Fig. 5). The saturation magnetization (M_s) values of Fe_3O_4 and nano-kaolin/Ti^{4+}/Fe_3O_4 were 50 and 23 emu g^{-1}, respectively. Although the magnetization of the catalyst is lower than that of Fe_3O_4, the proposed catalyst can be easily separated from the solution using an external magnet.

The X-ray diffraction (XRD) pattern of nano-kaolin/Ti^{4+}/Fe_3O_4 is shown in Fig. 6. According to the XRD pattern, the signals at $2\theta = 13°$, 20°, 25°, 41°, 46°, 61° and 68° indicate the

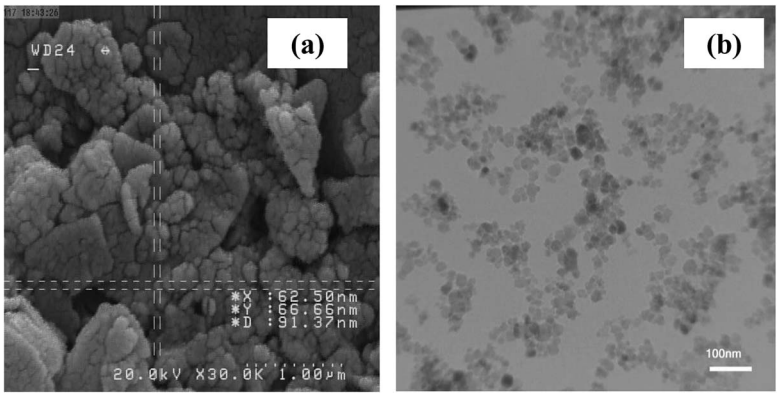

Fig. 2 (a) FE-SEM and (b) TEM images of nano-kaolin/Ti^{4+}/Fe_3O_4.

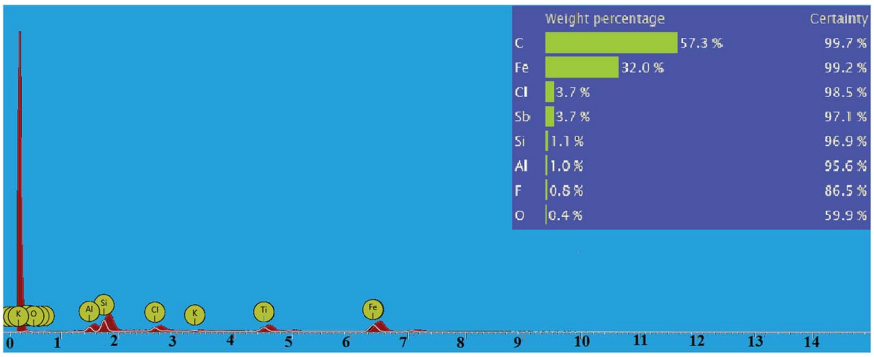

Fig. 3 The EDX spectra of nano-kaolin/Ti^{4+}/Fe_3O_4.

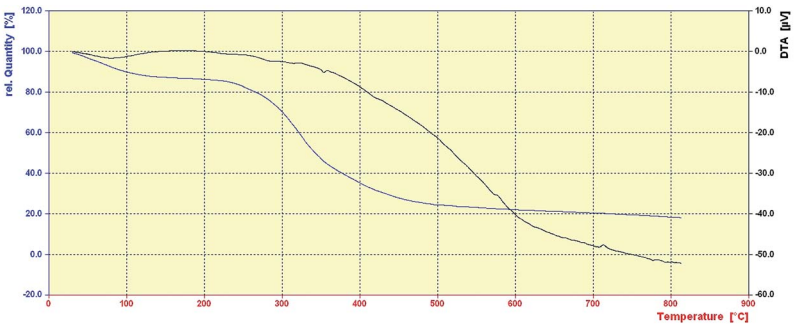

Fig. 4 Thermal gravimetric analysis of nano-kaolin/Ti^{4+}/Fe_3O_4.

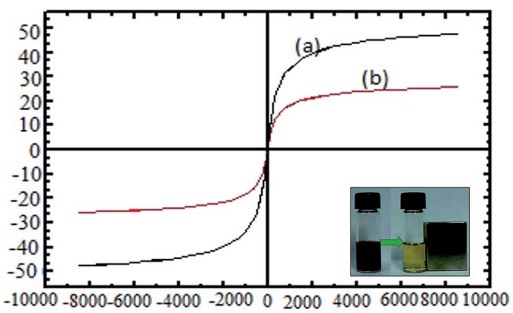

Fig. 5 Magnetization loops of (a) Fe_3O_4 and (b) nano-kaolin/Ti^{4+}/Fe_3O_4.

presence of kaolin. The four signals at $2\theta = 21°$, 27°, 39° and 50° indicate the existence of SiO_2. Moreover, the signals at 2θ = 31°, 36°, 44°, 58° and 63° are related to Fe_3O_4. Presumably, three other peaks at the 2θ value of 37°, 43° and 55° revealed that Ti was bonded to kaolin and Fe_3O_4.

The catalytic activity of the catalyst was investigated for the synthesis of 4*H*-pyrimido[2,1-*b*]benzothiazole using the three-component reaction of β-keto ester, aromatic aldehydes and 2-aminobenzothiazole. To select optimum conditions, the reaction of ethyl acetoacetate, benzaldehyde and 2-amino benzothiazole was studied as a model reaction under different conditions. According to Table 1, the best

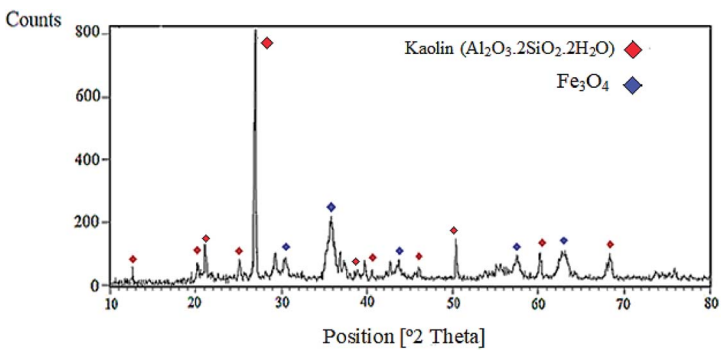

Fig. 6 XRD pattern of nano-kaolin/Ti^{4+}/Fe_3O_4.

Table 1 The reaction of 2-aminobenzothiazole, benzaldehyde and ethyl acetoacetate in the presence of nano-kaolin/Ti^{4+}/Fe_3O_4 under various conditions[a]

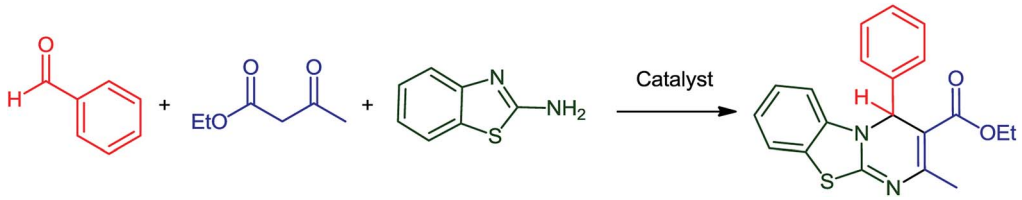

Entry	Catalyst (g)	Solvent/condition	Time (h)	Yield[b] (%)
1	Fe_3O_4 (0.03)	—/100 °C	1.5	52
2	Kaolin (0.03)	—/100 °C	1.5	72
3	Nano-kaolin/Ti^{4+} (0.03)	—/100 °C	1.5	78
4	Catalyst[c] (0.03)	H_2O/reflux	3	50
5	Catalyst[c] (0.03)	C_2H_5OH/reflux	4	30
6	Catalyst[c] (0.03)	—/80 °C	2	82
7	Catalyst[c] (0.03)	—/90 °C	2	75
8	Catalyst[c] (0.03)	—/110 °C	1.5	95
9	Catalyst[c] (0.025)	—/100 °C	1.5	65
10	Catalyst[c] (0.03)	—/100 °C	1.5	95
11	Catalyst[c] (0.04)	—/100 °C	1.5	78

[a] The amount ratios of 2-aminobenzothiazole (mmol), benzaldehyde (mmol) and ethyl acetoacetate (mmol) equals to 1 : 1 : 1. [b] Isolated yield. [c] Nano-kaolin/Ti^{4+}/Fe_3O_4.

conditions for the synthesis of 4*H*-pyrimido[2,1-*b*]benzothiazole under solvent-free conditions correspond to the utilization of 0.03 g of catalyst at 100 °C.

According to the conditions optimized for the model reaction, 4*H*-pyrimido[2,1-*b*]benzothiazole derivatives were synthesized by the reaction of various aromatic aldehydes,

Table 2 The synthesis of 4*H*-pyrimido[2,1-*b*]benzothiazole derivatives[a]

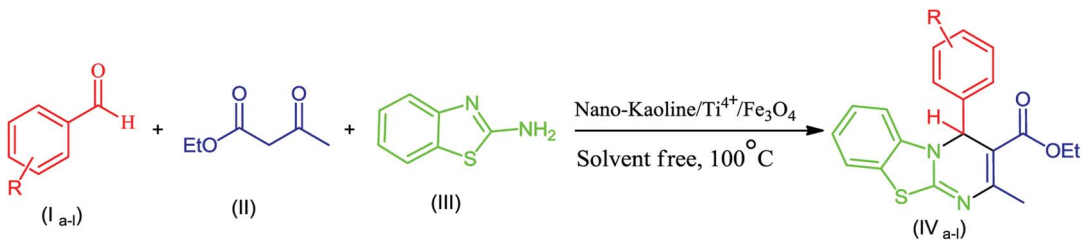

Entry	R	Product	Time (h)	Yield[b] (%)	Melting point		Ref.
					Observed	Reported	
1	H	IV_a	1.5	95	178–180	178–180	23
2	4-NO_2	IV_b	0.5	98	172–173	170–172	30
3	4-Cl	IV_c	2.2	95	141–143	140–142	15
4	4-Br	IV_d	1.6	92	111–113	110–114	31
5	4-OH	IV_e	3	90	210–214	110–112	30
6	2-NO_2	IV_f	1	50	120–124	123–125	14
7	2-Cl	IV_g	2.2	78	131–133	130–132	17
8	3-NO_2	IV_h	0.5	80	222–224	222–224	23
9	3-OH	IV_i	1.25	94	259–261	260–263	12
10	2,4-$(Cl)_2$	IV_j	1.4	70	133–135	133–135	13
11	2-OEt	IV_k	1.1	85	170–172	171–173	12
12	3,4-$(OH)_2$	IV_l	0.9	60	227–229	225–227	15

[a] One mmol of 2-aminobenzothiazole, aldehyde and ethyl acetoacetate was used. [b] Isolated yield.

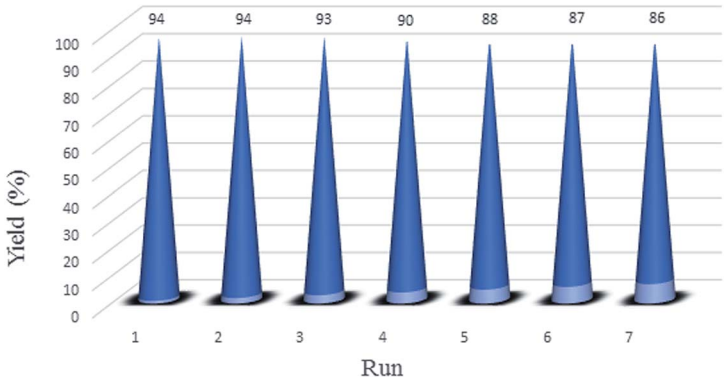

Fig. 7 The reusability experiment data of the catalyst.

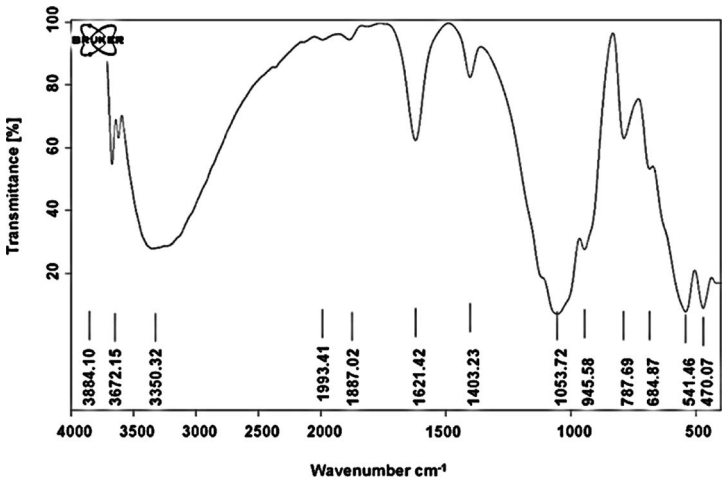

Fig. 8 The FTIR spectrum of the reused catalyst.

2-aminobenzothiazole and ethylacetoacetate in the presence of the nano-kaolin/Ti^{4+}/Fe_3O_4 catalyst. Based on the results tabulated in Table 2, the effects of the electron and the nature of the substituent on aldehyde significantly affected the time and yield of the reaction. The presence of electron-withdrawing groups in aryl aldehyde rings increased the activity of the aldehyde group and their yields were compared with that of electron-donating groups; the structure of the product was identified using melting point, FTIR, and ^{1}H-NMR spectral results.

To investigate the recovery and reuse function of nano-kaolin/Ti^{4+}/Fe_3O_4, the catalyst was used for seven times in the model reaction under identical conditions. After using the catalyst in the model reaction, it was isolated by an external magnet, washed with ethanol and then dried at room temperature. The results indicate that the catalyst nano-kaolin/Ti^{4+}/Fe_3O_4 can be reused without any significant loss of its catalytic activity (Fig. 7). The FTIR spectrum of the reused catalyst shows that there is no change in the catalyst structure during the recovery process (Fig. 8).

The proposed mechanism for the synthesis of 4*H*-pyrimido[2,1-*b*]benzothiazoles is shown in Scheme 2. In this reaction, the Ti^{4+} cation in the catalyst acts as a Lewis acid and activates the carbonyl groups in the substrates. At first, the aldehyde (I) as an electrophile and β-keto esters (II) as active methylene compounds produce the alkene (IV) *via* the Knoevenagel reaction. Then, the 2-aminobenzothiazole (III) reacts with the alkene (IV) *via* a Michael addition reaction, and an iminium ion (V) is formed. Subsequently, using proton transfer and intramolecular cyclization, the 4*H*-pyrimido[2,1-*b*]benzothiazole derivative(VII) is formed.

To investigate the performance of the nano-kaolin/Ti^{4+}/Fe_3O_4 catalyst in synthesis of 4*H*-pyrimido[2,1-*b*]benzothiazole derivatives, condensation of benzaldehydes, 2-aminobenzothiazole and ethyl acetoacetate was employed as the model reaction, and the results were compared with those obtained using other reported catalysts. The results of this study are shown in Table 3. According to the obtained results, the nano-kaolin/Ti^{4+}/Fe_3O_4 is one of the best catalyst for this purpose.

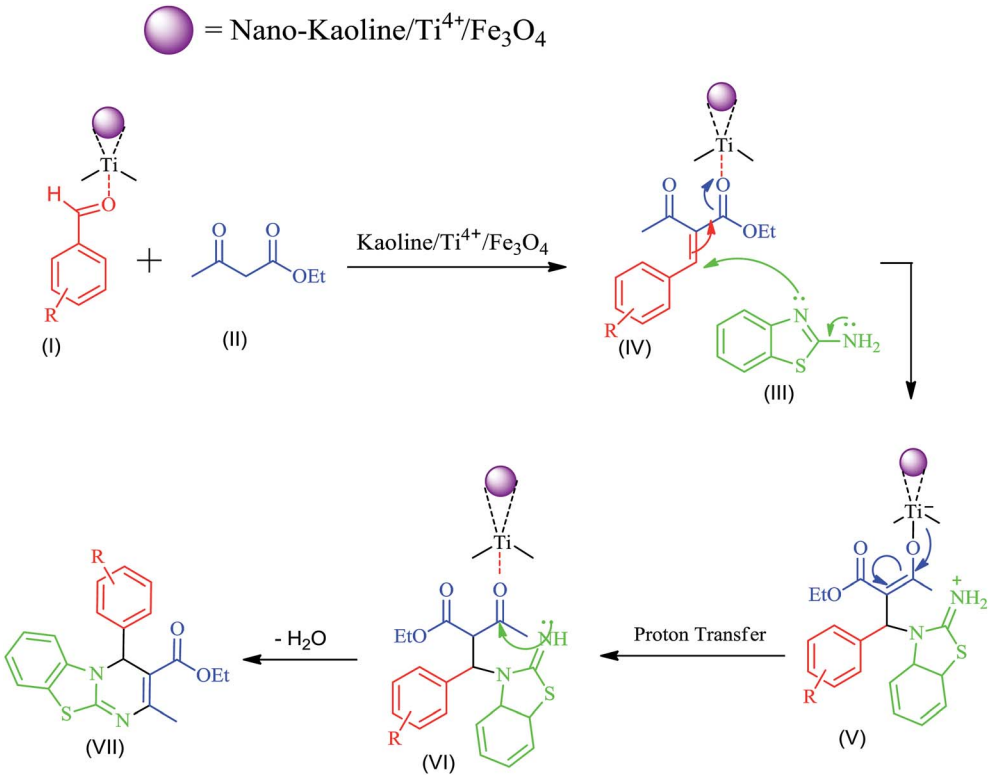

Scheme 2 A proposed mechanism for the preparation of 4*H*-pyrimido[2,1-*b*]benzothiazole derivatives.

Table 3 Comparison of the nano-kaolin/Ti^{4+}/Fe_3O_4 catalyst with other reported catalysts for the synthesis of ethyl-2-methyl-4-(phenyl)-4*H*-pyrimido[2,1-*b*][1,3]benzothiazole-3-carboxylate[a]

Entry	Catalyst	Solvent/condition	Time (h)	Yield[b] (%) (ref.)
1	TMGT[c] (0.08 g)	—/100 °C	5	66 (31)
2	TBAHS[d] (10 mol%)	Ethylene glycol/120 °C	2	83 (17)
3	Acetic acid (10 mol%)	Methanol/reflux	12	65 (32)
4	$AlCl_3$ (10 mol%)	—/60 °C	1.2	79 (30)
5	FeF_3 (10 mol%)	—/80 °C	2	85 (33)
6	Nano-cellulose/BF_3/Fe_3O_4 (0.06 g)	—/100 °C	1	80 (14)
7	Nano-kaolin/$TiCl_4$/Fe_3O_4 (0.03 g)	—/100 °C	1.5	95 (this work)

[a] One mmol of any substrate (2-aminobenzothiazole, benzaldehyde and ethyl acetoacetate) was used. [b] Isolated yield. [c] 1,1,3,3-*N*,*N*,*N*′,*N*′-Tetramethylguanidinium trifluoroacetate. [d] Tetrabutylammonium hydrogen sulfate.

Conclusion

Due to the importance of green chemistry, we have introduced the preparation and characterization of nano-kaolin/Ti^{4+}/Fe_3O_4 as a novel, eco-friendly and magnetically recyclable heterogeneous catalyst. This catalyst was used to synthesize 4*H*-pyrimido[2,1-*b*]benzothiazole derivatives *via* the one-pot three-component reaction of 2-aminobenzothiazole, aldehydes and ethyl acetoacetate under solvent-free conditions at 100 °C. Some of the important advantages of this protocol include short reaction times, high yields, easy work-up procedure and easy separation of the catalyst with reusability.

Experimental

General remarks

A Bruker (DRX-400 Avance) NMR spectrometer was used to obtain the NMR spectra. FTIR spectra were obtained using the Bruker, Equinox 55 spectrometer. Melting points were determined by the Buchi melting point B-540 B.V.CHI apparatus. Field emission scanning electron microscopy (FE-SEM) was carried out *via* Mira 3-XMU, and transmission electron microscopy (TEM) was conducted using Philips CM120 with the LaB_6 cathode and the accelerating voltage of 120 kV. The X-ray diffraction (XRD) pattern was obtained by the Philips X'pert MPD diffractometer equipped with a Cu Kα anode (k =

1.54 Å) in the 2θ range from 10° to 80°. The VSM measurements were performed using a vibrating sample magnetometer (Meghnatis Daghigh Kavir Co. Kashan, Iran). The thermogravimetric analysis (TGA) was conducted by NETZSCH TG 209 F1 Iris. Energy-dispersive X-ray spectroscopy (EDS) of the catalyst was conducted by the EDS instrument Phenom pro X.

Preparation of the Fe_3O_4 NPs

A mixture of $FeCl_3 \cdot 6H_2O$ (2.7 g, 10 mmol) and $FeCl_2 \cdot 4H_2O$ (1 g, 5 mmol) in deionized water (25 ml) was heated until 80 °C. Then, 17 ml of NH_3 (30%) was added slowly. The mixture was stirred using a mechanical stirrer for 30 minutes. Then, black magnetic nanoparticles were deposited using an external magnet and washed three times with deionized water. Finally, the Fe_3O_4 NPs were dried at 80 °C for 4 hours.

Preparation of nano-kaolin/Ti^{4+}

In a beaker, 1 ml of $TiCl_4$ was added dropwise to a mixture of nano-kaolin (2 g) in 10 ml of dichloromethane and stirred using a mechanical stirrer for 1 h at room temperature. The obtained suspension was filtered, washed with dichloromethane and dried at room temperature.

Preparation of nano-kaolin/Ti^{4+}/Fe_3O_4

At first, a mixture of nano-kaolin/Ti^{4+} (2 g) and dichloromethane (10 mL) was placed in an ultrasonic bath for 30 minutes. Then, nano-Fe_3O_4 (1 g) was added to the mixture and placed in the ultrasonic bath for 40 minutes to disperse the particles. The resulting suspension was obtained by an external magnet, washed with dichloromethane, and dried at room temperature.

General procedure for the synthesis of 4*H*-pyrimido[2,1-*b*] benzothiazole derivatives

In a sand bath, a mixture of aldehyde (1 mmol), ethyl acetoacetate (1 mmol), 2-aminobenzothiazole (1 mmol) and nano-kaolin/Ti^{4+}/Fe_3O_4 (0.03 g) was heated to 100 °C. The right time for the completion of the reactions is shown in Table 2. After completion of the reaction, the reaction mixture was dissolved in ethanol, and the catalyst was separated by an external magnet. Finally, water was added to the residue, and the product appeared as a pure solid. For the recovery of the catalyst, the magnetically resolved catalyst was washed with ethanol at least three times and then dried at room temperature.

Conflicts of interest

There are no conflicts to declare.

Acknowledgements

The Research Council of Yazd University is gratefully acknowledged for the financial support for this work.

References

1 Z. Y. Yu, Q. S. Fang, J. Zhou and Z. B. Song, *Res. Chem. Intermed.*, 2016, **42**, 2035.
2 M. S. Chaitanya, G. Nagendrappa and V. P. Vaidya, *J. Chem. Pharm. Res.*, 2010, **2**, 206.
3 A. Y. Hassan, *Phosphorus, Sulfur Silicon Relat. Elem.*, 2009, **184**, 2856.
4 M. T. Gabr, N. S. El-Gohary, E. R. El-Bendary and M. M. El-Kerdawy, *Eur. J. Med. Chem.*, 2014, **85**, 576.
5 D. V. Kashinath, Y. M. Rajmani and C. S. Ravindra, *J. Pharma Res.*, 2013, **6**, 574.
6 V. K. Deshmukh, P. Raviprasad, P. A. Kulkarni and S. V. Kuberkar, *Int. J. ChemTech Res.*, 2011, **3**, 136.
7 M. A. El-Sherbeny, *Arzneim.-Forsch./Drug Res.*, 2000, **50**, 848.
8 M. M. M. Gineinah, *Sci. Pharm.*, 2001, **69**, 53.
9 M. Yadav, V. K. Deshmukh and S. R. Chaudhari, *Int. J. Pharm. Sci. Rev. Res.*, 2013, **22**, 41.
10 S. Maddila, S. Gorle, N. Seshadri, P. Lavanya and S. B. Jonnalagadda, *Arabian J. Chem.*, 2016, **9**, 681.
11 S. R. Vaidya and J. J. Chamergore, *Chem. Biol. Interface*, 2016, **6**, 47.
12 S. Azad and B. F. Mirjalili, *RSC Adv.*, 2016, **6**, 96928.
13 S. Azad and B. F. Mirjalili, *Res. Chem. Intermed.*, 2017, **43**, 1723.
14 B. F. Mirjalili and F. Aref, *Res. Chem. Intermed.*, 2018, **44**, 4519.
15 S. A. Fazeli-Attar and B. F. Mirjalili, *Res. Chem. Intermed.*, 2018, **44**, 6419.
16 P. K. Sahu, P. K. Sahu and D. D. Agarwal, *RSC Adv.*, 2013, **3**, 9854.
17 L. Nagarapu, H. K. Gaikwad, J. D. Palem, R. Venkatesh, R. Bantu and B. Sridhar, *Synth. Commun.*, 2013, **43**, 93.
18 Q. Zhang, W. Tongamp and F. Saito, *Powder Technol.*, 2011, **212**, 354.
19 H. H. Murray, *Appl. Clay Sci.*, 2000, **17**, 207.
20 A. M. Doyle, T. M. Albayati, A. S. Abbas and Z. T. Alismaeel, *Renewable Energy*, 2016, **97**, 19.
21 A. H. Lu, E. E. Salabas and F. Schüth, *Angew. Chem., Int. Ed.*, 2007, **46**, 1222.
22 X. Batlle and A. Labarta, *J. Phys. D: Appl. Phys.*, 2002, **35**, R15.
23 R. Narayanan, Ch. Tabor and M. A. El-Sayed, *Top. Catal.*, 2008, **48**, 60.
24 L. Xu, L.-M. Yang and E. Ganz, *Theor. Chem. Acc.*, 2018, **137**, 98.
25 J.-H. Liu, L.-M. Yang and E. Ganz, *J. Mater. Chem. A*, 2019, **7**, 11944.
26 J.-H. Liu, L.-M. Yang and E. Ganz, *J. Mater. Chem. A*, 2019, **7**, 3805.
27 J.-H. Liu, L.-M. Yang and E. Ganz, *ACS Sustainable Chem. Eng.*, 2018, **6**, 15494.
28 S. Azad and B. F. Mirjalili, *Mol. Diversity*, 2019, **23**, 413.

29 B. F. Mirjalili, A. Bamoniri and L. Asadollah Salmanpoor, *J. Nanostruct.*, 2018, **8**, 276.
30 P. K. Sahu, P. K. Sahu, J. Lal, D. Thavaselvam and D. D. Agarwal, *Med. Chem. Res.*, 2012, **21**, 3826.
31 A. Shaabani and A. Maleki, *Appl. Catal., A*, 2007, **331**, 149.
32 P. K. Sahu, P. K. Sahu, Y. Sharma and D. D. Agarwal, *J. Heterocycl. Chem.*, 2014, **51**, 1193.
33 A. B. Atar, Y. S. Jeong and Y. T. Jeong, *Tetrahedron*, 2014, **70**, 5207.